Bent-core liquid crystals forming two- and three-dimensional modulated structures

J. Szydlowska,[1] J. Mieczkowski,[1] J. Matraszek,[1] D. W. Bruce,[2] E. Gorecka,[1,3] D. Pociecha,[1] and D. Guillon[3]
[1]*Chemistry Department, Warsaw University, Al. Zwirki i Wigury 101, 02-089 Warsaw, Poland*
[2]*School of Chemistry, University of Exeter, Stocker Road, Exeter EX4 4QD, United Kingdom*
[3]*GMO, Institute of Physics and Chemistry of Materials of Strasbourg, Strasbourg, France*
(Received 14 October 2002; published 12 March 2003)

Two columnar phases of bent-core molecules have been observed, with a two-dimensional (2D) structure modulated in the plane perpendicular to the direction of the spontaneous polarization vector. The phases are switchable under an applied electric field, contrary to the commonly observed 2D modulated B_1 phase. These new phases are built from broken smectic layers with orthogonal or tilted molecules. The evidence for a 3D structure in which the density modulations along and perpendicular to the spontaneous polarization vector co-exists is also given.

DOI: 10.1103/PhysRevE.67.031702 PACS number(s): 61.30.Cz, 61.30.Eb, 61.30.Gd

Bent-core (banana) mesogens, in common with rodlike mesogens, readily form lamellar structures, i.e., phases with one-dimensional (1D) density modulation [1]. The most studied smectic phase made of bent-core molecules is the B_2 phase [2]. Due to their bent shape, molecules cannot rotate freely, resulting in long-range correlation of molecular dipole moments and thus, in ferroelectricity in the single smectic layer. In the multilayer structure, the compensation of spontaneous electric polarization ($\mathbf{P}_s$) is obtained by the antiferroelectric arrangement of neighboring layers.

The alternative route by which the system can avoid bulk spontaneous polarization is by breaking the layers and forming 2D or even 3D modulated structures. Columnar 2D modulated phases made of broken layers are known for many classes of mesogenic compounds e.g., rodlike molecules with strongly polar terminal groups [3] or polycatenar compounds [4]. However, for bent-core molecules, since there are three competing order parameters: density modulation, tilt and polarization, a more complex variety of phases can be obtained. The most frequently observed 2D modulated phase made of bent-core molecules is the columnar B_1 phase [5] with density modulation in the plane parallel to the $\mathbf{P}_s$ vector [Fig. 1(a)]. This phase has an antiferroelectric crystallographic unit cell and is reported as being nonswitchable. However, it is also feasible that density modulations could be formed in the plane perpendicular to $\mathbf{P}_s$ vector [Fig. 1(b)] and such a structure has been already suggested for dimeric compounds [6]. We will show that this phase, which will be designated as reversed B_1 ($B_{1\mathrm{Rev}}$), when made of rigid, bent-core molecules is switchable and thus, has distinctly different polar and optical properties to the B_1 phase. In fact, we will show that two $B_{1\mathrm{Rev}}$ phases, with tilted or nontilted smectic layers, exist. Also, the case of a 3D structure will be discussed in which both mentioned density modulations, along and perpendicular to the $\mathbf{P}_s$ direction coexist.

The phase sequence for the studied materials [7] (Fig. 2) was determined by differential scanning calorimetry (Perkin Elmer DSC-7). The structure of the mesophases was elucidated by x-ray measurements (Cu-K_α radiation, patterns registered with Inel CPS 120 curved counter or Guinier camera setup). For all phases studied, a diffuse signal is observed in the high-angle region, corresponding to an average distance of 4.5 Å and pointing to the existence of liquidlike correlations. In the low-angle region, however, few signals were observed (Table I) that exclude a simple 1D lamellar structure.

The phase formed by compound 1 has been identified previously as the B_1 phase [8] built of columns formed by layer fragments, and it exhibits density modulations in the plane parallel to $\mathbf{P}_s$ vector. The x-ray pattern of the B_X phase, found for compound 2, was similar to that observed for the B_1 phase of compound 1 and matched a 2D rectangular centered lattice [Fig. 3(a)]. For both the B_1 and B_X phases, one of the crystallographic lattice parameters, *b*, is close to the molecular length. This length was estimated by molecular modeling (HYPERCHEM software) and taken as shortest distance between molecular ends. The other dimension is *a*

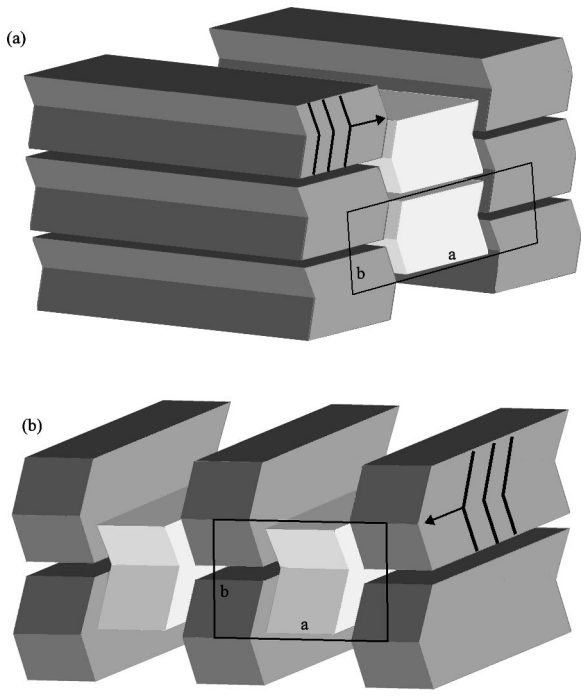

FIG. 1. Schematic drawing of (a) B_1 and (b) $B_{1\mathrm{Rev}}$ structures. Arrows indicate the P_s vector in the column, a and b are dimensions of the crystallographic unit cell.

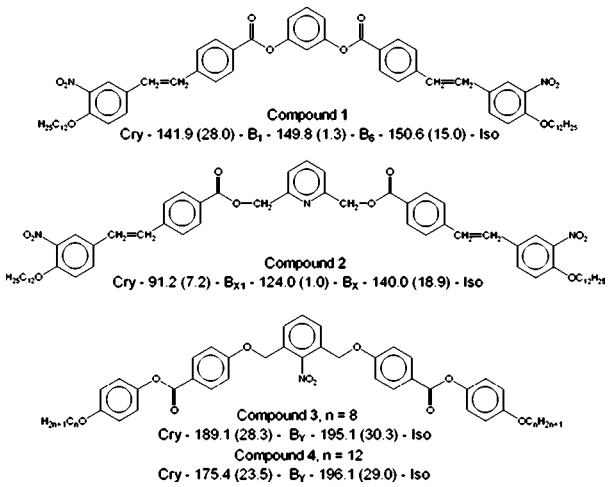

FIG. 2. Molecular structure of compounds 1-4 with the phase transition temperatures and enthalpy changes (in parentheses, $J\,g^{-1}$).

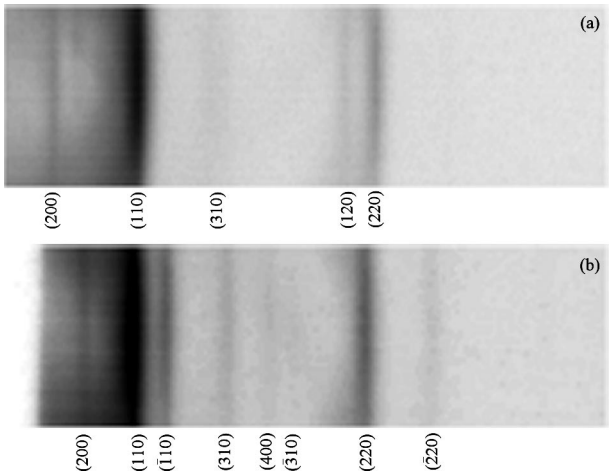

FIG. 3. Low-angle part of the x-ray images registered with a Guinier camera in the (a) B_X and (b) B_{X1} phase for compound 2.

$=112$ Å for B_1 phase and $a=154$ Å for the B_X phase. Assuming a density of 1 g/cm^3 and the average molecular distance along the column ~ 5 Å, the number of the molecules in the cross-section of the column can be estimated to be 9 and 12 in the B_1 and B_X phases, respectively. The x-ray patterns are nearly temperature independent within each phase temperature range. For compound 2, below the B_X phase, another columnar phase B_{X1}, for which x-ray reflections match the orthorhombic structure was found [Fig. 3(b)]. The dimensions a and b of the 2D crystallographic unit cell are slightly shorter than for the B_X phase, and the deviation from the rectangular shape of the crystallographic lattice is small—the tilt angle is about 10°.

The optical textures of the B_1 and B_X phases are similar (Fig. 4). They both exhibit pseudobroken fans or circular domains with extinction brushes directed along polarizing directions. The textures, obtained in a thin glass cell are of low birefringence. The birefringence, estimated from the

TABLE I. X-ray diffraction signals for B_1, B_X, B_{X1}, and B_Y phases and corresponding crystallographic distances.

	Signal indexes	(200)	(110)	(210)	(400)	(020) (120)	(220)						Cell dimensions
B_1	Measured distance (*A*)	55.8	46.4	38.1	27.6	24.9 25.4	23.0						$a=111.6$
	Calculated distance (*A*)	55.8	46.4	37.6	27.6	24.9	23.0						$b=53.5$
	Signal indexes	(200)	(110)	(310)	(020) (120)	(220)	(330) (430)	(440) (340)	(540)	(660)			$a=154.0$
Sm*X*	Measured distance (*A*)	77.0	50.5	37.0	26.2 26.7	24.5	16.2 16.8	12.8 12.5	12.2	8.4			$b=53.5$
	Calculated distance (*A*)	77.0	50.5	37.0	26.3	25.2	16.2	12.8	12.2	8.4			
	Signal indexes	(200)	(110)	($\bar{1}$10)	(310)	(400)	($\bar{3}$10)	(220) (020)	($\bar{2}$20)	(620)	(330)	(440)	$a=128.3$
SmX_1	Measured distance (*A*)	63.1	51.5	44.5	35.7	31.6	29.3	24.9 25.2	21.8	18.2	16.5	12.7	$b=51.8$
	Calculated distance (*A*)	63.1	51.5	44.5	35.8	31.6	29.8	25.4	22.2	17.9	16.8	12.6	$\alpha=79.6°$
	Signal indexes	(002)	(200)	(110)	Calculated cell dimensions								
Sm*Y*	Compound 3	82.8	71.3	38.9	$a=142.6$, $b=40.4$, $c=165.6$								
	Compound 4	87.5	70.0	45.3	$a=140.1$, $b=47.9$, $c=174.0$								

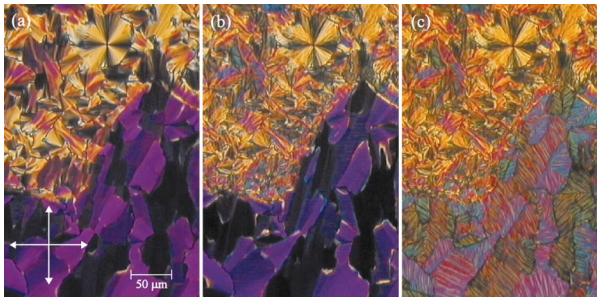

FIG. 4. (Color) Texture of the B_X and B_{X1} phases for compound 2 in a 4μ cell. The lower part of each picture shows the area between electrodes. The yellow/violet color corresponds to the birefringence $\Delta n = 0.08/0.15$. (a) The B_X phase after applying a weak (about 7 V/μm) pulse electric field, (b) the switch-on state of the B_{X1} phase, (c) the switch-off state of the B_{X1} phase. The arrows indicate the polarizer and analyzer directions.

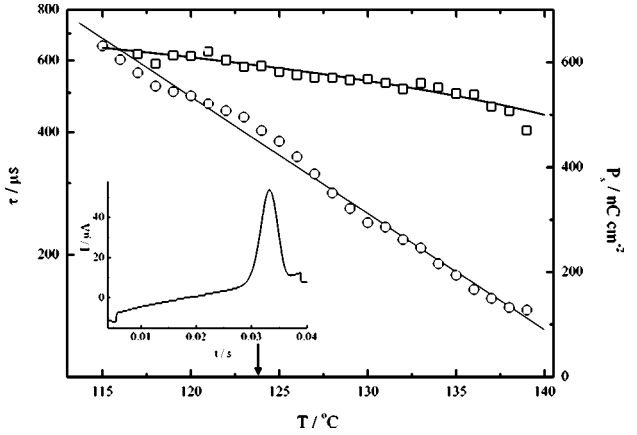

FIG. 5. Temperature dependence of spontaneous polarization (squares) and switching time (circles) for compound 2. The arrow indicates the B_X-B_{X1} transition temperature. Inset: the switching current peak registered in the B_X phase.

tabulated interference colors of quartz wedge, was $\Delta n = 0.09$ for B_1 phase and $\Delta n = 0.08$ for B_X phase, suggesting that in both phases molecules are aligned with their banana planes on the glass surface. For compound **2** at the transition to the lower-temperature B_{X1} phase, the circular domains become broken and blurred, but the direction of the extinction brushes is preserved [Figs. 4(b) and 4(c)]. The texture changes are reminiscent of those observed at the Sm*A*-Sm*C* phase transition [9]. In the fanlike texture, small areas of distinctly higher birefringence ($\Delta n = 0.17$), seen in the B_X phase, grow in to the B_{X1} phase.

Despite similar textures of the B_1, B_X, and B_{X1} phases, their electrooptic properties are qualitatively different. Thus, when an electric field is applied to the B_1 phase, neither variation of birefringence nor switching current is recorded. However, both phases formed by compound 2 are responsive to an applied electric field. If a weak electric field (<10 V/μm) is applied to a freshly prepared sample, a sudden increase in birefringence to $\Delta n = 0.15$, as well as a reformation of the texture (Fig. 4) are observed. However, the light extinction directions parallel to the polarization directions remain unchanged, showing that the eigendirections of the refractive index ellipsoid are not affected by the field. The alterations are irreversible—removing the field does not restore the low birefringent, virgin texture. The texture reorganization under weak electric field is not accompanied by a polarization switching current. Thus, similar to the SmC_A phase, most probably this process is driven by the Freederiks transition [10] e.g., the dielectric anisotropy-electric field coupling, in which bent-core molecules reorient their planes from a parallel to a perpendicular orientation with respect to the glass surface.

The polarization switching current is detected in both the B_X and B_{X1} phases at significantly higher voltage (>15 V/μm) than that necessary to realign the virgin texture. Only a single current peak is registered even at low frequency, down to 1 Hz (Fig. 5 inset) that disappears in isotropic phase. The value of spontaneous electric polarization, $450-600$ nC/cm^2, is comparable to that reported for other banana phase B_2 (350–700 nC/cm^2) [1]. No peculiar optical change is detected at the voltage at which the switching current occurs. Upon increasing the dc electric field, no substantial texture reorganization is observed except for a small, reversible and continuous increase in birefringence (to $\Delta n = 0.16$), that reflects an increase in the orientational order. The threshold field that reverses the polarization as well as the spontaneous electric polarization and the switching time increase continuously with decreasing temperature, without any anomaly at the B_X-B_{X1} phase transition (Fig. 5). Moreover, when the low-temperature phase is formed under the electric field, the phase transition is not detected microscopically [Fig. 4(b)]. Thus, the new phase structure is built without molecular reorientation. When the field is removed in the low-temperature phase, the irregular stripe texture forms slowly. The high birefringence of these stripes $\Delta n = 0.16-0.17$ [Fig. 4(c)] shows that molecules are synclinic in neighboring smectic layers.

A contact sample with the compounds 1 and 2 was prepared. In the contact area the temperature range of the lamellar, intercalated B_6 phase [1], present in compound 1, strongly increases and the clearing temperature is strongly lowered. This suggest the phase diagram for binary mixture of compounds 1 and 2 in which B_1 and B_X phases are not miscible. This supports the conclusion that B_1 and B_X columnar phases have different structures.

In the dielectric studies all B_1, B_X, and B_{X1} phases reveal their antiferroelectric character. In the measured frequency range (20 Hz–300 kHz, Wayne Kerr Impedance Analyzer), there are no modes that are specific for the liquid crystalline phases. Only a single, weak ($\Delta\varepsilon \sim 10$) process with a relaxation frequency at $\sim 10^5$ Hz is found that varies continuously through the liquid crystalline as well as the isotropic phases. We assume that the mode arises from noncollective molecular rotations [11]. Since the phase is antiferroelectric, the single current peak detected in polarization measurements should be considered as two signals merged into one due to the long relaxation time necessary to restore the antiferroelectric state.

Summarizing, both the B_1 and B_X phases have centered, rectangular, crystallographic lattices and can be considered as made of broken, nontilted layers that form a 2D crystal-

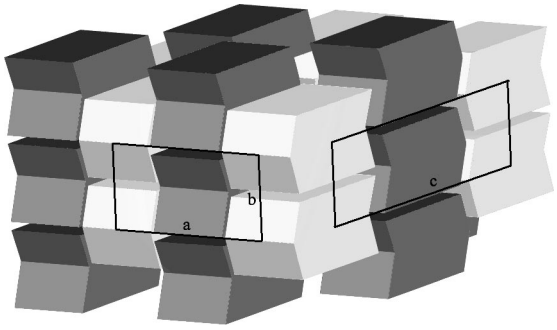

FIG. 6. Schematic structure of the 3D modulated phase.

lographic lattice. However, since the B_X phase is switchable, thus it has a different structure to the B_1 phase. We deduced that the density modulation wave in the B_X phase is perpendicular to the $\mathbf{P}_s$ direction [Fig. 1(b)], thus the phase is reversed B_1 phase ($B_{1\mathrm{Rev}}$). For the proposed structure the response to the electric field results from the collective rotation of molecules around their long axes without change in the column direction. A similar switching mechanism has been already reported for the nontilted, bent-core C_{PA} phase [12]. For the phase presented here, the size a of the crystallographic cell seems to be sufficiently large ($\sim$12 molecules) to consider one column as a fragment of C_{PA} phase layer. The steric hindrance coming from interactions between column boundaries do not limit the molecular rotation, contrary to the situation in the B_1 phase, in which switching would require breaking of the close-packing molecular structure. Considering that the B_{X1} phase is also switchable, that it has orthorhombic crystallographic unit cell and that it evolves from the nontiled $B_{1\mathrm{Rev}}$ phase, we conclude it is a reversed type phase $B_{1\mathrm{Rev\ Tilted}}$—built of tilted layers, like the synclinic B_2 phase. Since the transition between orthogonal and tilted phases under electric filed occurs without optical changes we deduced that at this transition the director is not changed, while the layers tilt. Moreover, the lack of textural change under electric field shows that the switching mechanism is different to that found in the B_2 phase. In the $B_{1\mathrm{Rev\ Tilted}}$ phase, under an electric field, the molecules adjust their dipole moments by rotation along their long axes, rather than by the rotation on the tilt cone. Since the ground state in $B_{1\mathrm{Rev\ Tilted}}$ phase is racemic but the switched on state is enantiomeric this process can be seen as field induced chirality.

As two, basic modulated structures exist, with the density modulation waves along $\mathbf{P}_s$ (B_1 phase) or perpendicular to $\mathbf{P}_s$ ($B_{1\mathrm{Rev}}$ phases), the question arises whether they both could be combined into a 3D periodic structure (Fig. 6)?

The x-ray pattern for the B_Y phase, found in compounds 3 and 4, seems to confirm such a possibility. In the low-angle region, three incommensurate diffraction signals were registered. The strongest one is close to the molecular dimension, while the two others, of low intensity, correspond to distances much larger than molecular length (Table I). This suggests a three-dimensional phase structure. The main signal can be indexed as $(110)=(011)$, while two weaker signals, (200) and (002), correspond to modulation waves along two orthogonal directions. One of the possible structures, that seems to be the most probable due to close-packing conditions, can be obtained by breaking the columns of the $B_{1\mathrm{Rev}}$ phase along the (001) direction into parts with length given by the (002) periodicity (Fig. 6). However, the texture observation suggest even a more complicated structure which additionally involves the anticlinic arrangement of molecules. The virgin texture of the B_Y phases is of focalconic and it shows electrooptical properties similar to the $B_{1\mathrm{Rev}}$ phase. At low electric field (<15 V/μm) the Freederiks transition takes place, in which the birefringence increases from $\Delta n = 0.05$ to 0.07. Thus, the field-induced birefringence is much lower than that observed for compound 2, which excludes a synclinic or orthogonal structures. An applied triangular voltage produces a polarization switching current ($\mathbf{P}_s \approx 450$ nC/cm^2), which is not accompanied by further optical changes. The low birefringence of *field-on* and *field-off* states suggests that both states have an anticlinic structure. The assumption of anticlinic arrangement is also supported by the observation that a one-surface-free sample showing a focalconic texture, at certain temperature is not birefringent (Fig. 7). The focal-conic texture indicates that the layers are perpendicular to the glass substrate, while the free surface forces the planes of the bent-core molecules to be perpendicular to the air—LC boundary. To obtain zero birefringence for such a sample, the molecules should be anticlinic in subsequent columns or layers and have 45° tilt from the layer normal [13]. A possible B_Y phase organization could be the structure shown in Fig. 6, however, built from tilted molecular blocks which are formed from molecules tilted toward their side. Along the (001) direction the subsequent blocks should have alternating tilt direction. Since the tilt is temperature dependent, the zero birefringence could be obtained when the tilt reaches 45°.

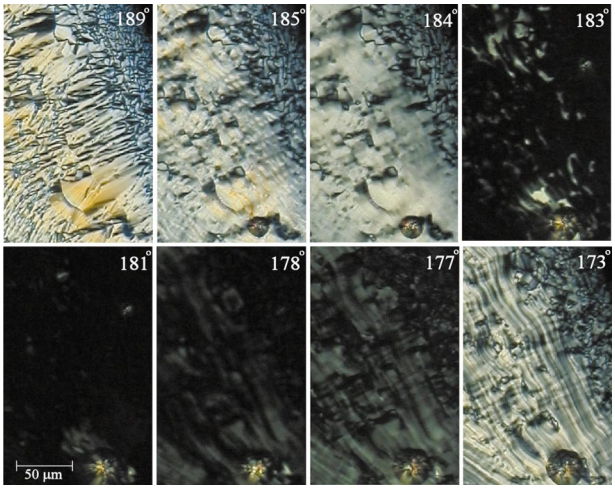

FIG. 7. (Color) The sequence of the pictures, showing the focalconic texture obtained with one-surface-free sample for compound 3, on lowering temperature. In temperatures around 180°, zero birefringence suggests anticlinic structure of the 3D modulated phase with 45° tilt angle.

In conclusion, it seems that the bent-shaped molecules easily form two types of 2D modulated structures in which the density modulations are in the plane parallel or perpendicular to the spontaneous electric polarization vector. The direction of the density modulation is defined by the type of

blocks that are formed by bent-shaped molecules. If the molecules prefer to organize into blocks with the infinite dimension in the direction of the banana tip, the $B_{1\mathrm{Rev}}$ phase is formed. In contrast, the columns with the infinite dimension in the direction perpendicular to the banana plane are organized into the B_1 type phase. Considering the attractive van der Waals molecular interactions, the latter case seems to be more probable for bent-core molecules that are almost flat e.g., the phenyl moieties in banana branches are nearly coplanar with the central ring. It is the case of compound 1, where branches are linked to the central unit by the ester groups, that have low flexibility. The molecules with the phenyl moieties in banana branches twisted with respect to the plane of the central ring would prefer to stack along the direction of banana arrow. It is possible when links at central phenyl ring are rather flexible, that take place for compound 2. If none of these situations is dominating the blocks of finite dimensions in both directions can be formed, that leads to appearance of 3D modulated phases. The type of the phases formed by compounds 1-4 seems to be consistent with the above idea.

We would like to thank Dr. Mojca Cepic for many fruitful discussions and the EU for support provided to J. Matraszek through the Marie Curie Training Site PODEUMM, Contract No. HPMT-2000-00016.

[1] G. Pelzl, S. Diele, and W. Weissflog, Adv. Mater. **9**, 707 (1999).

[2] T. Niori, T. Sekine, J. Watanabe, T. Furukawa, and H. Takezoe, J. Mater. Chem. **6**, 1231 (1996); D.R. Link, G. Natale, R. Shao, J.E. Maclennan, N.A. Clark, E. Korblova, and D.M. Walba, Science **278**, 1924 (1997).

[3] G. Sigaud, F. Hardouin, M.F. Achard, and A.M. Levelut, J. Phys., **42**, 107 (1981); F. Hardouin, H.T. Nguyen, M.F. Achard, and A.M. Levelut, J. Phys. (France) Lett. **43**, L-32 (1982); A.M. Levelut, *ibid.* **45**, L-603 (1984); J. Prost, J. Phys. (Paris) **40**, 581 (1979); J. Prost and P. Barois, J. Chem. Phys. **80**, 65 (1983).

[4] Nutz, S. Diele, G. Pelzl, H. Ringsdorf, W. Paulus, and G. Willson, Liq. Cryst. **18**, 699 (1995); S. Diele, K. Zierbarth, G. Pelzl, D. Demus, and W. Weissflog, *ibid.* **8**, 211 (1990).

[5] J. Watanabe, T. Niori, T. Sekine, and H. Takezoe, Jpn. J. Appl. Phys., Part 1 **37**, L139 (1998).

[6] Y. Takanishi, T. Izumi, J. Watanabe, K. Ishikawa, H. Takezoe, and A. Iida, J. Mater. Chem. **9**, 2771 (1999).

[7] The synthesis and chemical analysis for the compounds will be described elsewhere.

[8] J. Mieczkowski, J. Szydlowska, J. Matraszek, D. Pociecha, E. Gorecka, B. Donnio, and D. Guillon, J. Mater. Chem. **12**, 3392 (2002).

[9] G. W. Gray, and J. W. G. Goodby, *Smectic Liquid Crystals: Textures and Structures* (Leonard Hill, Glasgow, 1984).

[10] Bing Wen, Shiyong Zhang, S.S. Keast, M.E. Neubert, P.L. Taylor, Ch. Rosenblatt, Phys. Rev. E **62**, 8152 (2000).

[11] H. Scmalfuss, D. Shen, C. Tschierske, and H. Kresse, Liq. Cryst. **26**, 1767 (1999).

[12] A. Eremin, S. Diele, G. Pelzl, H. Nadasi, W. Weissflog, J. Salfetnikova, and H. Kresse, Phys. Rev. E **64**, 051707 (2001).

[13] K. D'have, P. Rudquist, S.T. Lagerwall, H. Pauwels, W. Drzewinski, and R. Dabrowski, Appl. Phys. Lett. **76**, 3528 (2000); K. D'have, A. Dahlgren, P. Radquist, J.P.P. Lagerwall, G. Andersson, K. Matuszczyk, S.T. Lagerwall, R. Dabrowski, and W. Drzewinski, Ferroelectrics **244**, 415 (2000).